in vivo *26*: 599-608 (2012)

Review

Fluorescent Protein-based Tumor Models

V. YAGUBLU[1,2], Z. AHMADOVA[1], M. HAFNER[3,4] and M. KEESE[1,5]

[1]*Surgical Clinic, University Medical Center Mannheim, Mannheim, Germany;*
[2]*Scientific Center of Surgery, Baku, Azerbaijan;*
[3]*Institute for Molecular and Cell biology, Mannheim University of Applied Sciences, Mannheim, Germany;*
[4]*Institute for Medical Technology, University Heidelberg Heidelberg University and Mannheim University of Applied Sciences, Mannheim, Germany;*
[5]*Clinic for Vascular and Endovascular Surgery, Johann Wolfgang Goethe University Hospital, Frankfurt, Germany*

Abstract. *Numerous animal models have been developed to provide a deeper insight to tumor progression in the search for new therapeutic leverage. The closer the tumor model represents the real tumor disease, the better. The ideal model provides monitoring, tumor cell detection and quantification, and the physiological events involved in tumor progression and tumor dissemination, simultaneously. Sensitive techniques have been developed which involve fluorescent protein-based methods, developed in order to quantify the tumor cells in a whole organ, and in parallel, to visualize the cells. These genetically encoded fluorescent proteins may also be used to develop biological sensors to monitor the physiological reaction of tumor cells within whole organs in living animals. Here, we aim to review past and present work and to show the perspectives of animal models involving fluorescent protein-transfected tumor cells.*

In general, a model for a human disease remains by definition only an imperfect representation of the real disease. A multitude of *in vitro* and *in vivo* models have been developed. These models have made a tremendous contribution to the understanding of tumor biology and have lead to new and novel approaches in both cancer treatment and prevention. Effective modeling of tumor started with the invention of cell culture systems. Murine sarcoma-180 cells were the first tumor cells to be cultured and passaged. This is why cell culture media components and supplements, such as fetal bovine serum, had to be optimized (1).

In early cancer research, cell lines were mostly used for growth inhibition assays, where the cells were cultured in the presence of drugs. Nowadays, cell cultures can be used to study a variety of aspects of tumor growth, tumor angiogenesis, tumor invasion and immune cell interactions. Despite their convenience, conventional cell culture assays which use monolayers of cells fail to model important features of solid tumors by forcing the cells to adopt to an unnatural environment (2). Since most tumors are diffusion-limited with slow and variable blood flow, monolayer cultures cannot mimic this important feature of the tumor tissues (3). To overcome this inconvenience, several three-dimensional tissue culture systems have been developed that allow cells to grow in a more realistic manner (2, 4, 5). Tumor vasculature as one component of tumor angiogenesis is one of the stromal components which can be exploited as a drug target. On these grounds, assays for endothelial cell migration, differentiation assays and organ culture assays have been developed (6, 7). Comparison of findings from different experiments remains a difficult topic due to differences in the source, viability and passage number of the cells used in these assays. Another elegant model to study tumor cell angiogenesis is the chick chorioallantoic membrane assay. In this assay, a window is carefully cut in an egg shell and tumor cells can then be implanted (8). Thus the development of tumor vasculature may be studied in the context of the immature immune system of a 7 to 8-days-old chicken embryo (9).

Currently, no available tumor cell culture system is able to closely model human disease. *In vivo* models represent an alternative. Findings which are derived from *in vivo* models are mostly more relevant for the treatment of human tumors.

The first *in vivo* models were developed in the mid-1960s: the murine leukemia models P388 and L1210 were selected

Abbreviations: FP: Fluorescent proteins, GFP: Green fluorescent protein.

Correspondence to: Michael Keese, Klinik für Gefäss.- und Endovaskularchirurgie, Klinikum der Johann Wolfgang Goethe Universität Frankfurt, Germany. E-mail: Michael.Keese@kgu.de

Key Words: Tumor model, fluorescence, GFP, FRET, biosensor, review.

as the initial systems in which potential agents could be tested for antitumoral activity before further development (10). Syngenic tumor models, which use implanted tumor cells that are derived from the strain in which the tumor originated (11, 12), offer certain scientific and practical valuable advantages: they are reproducible, grow in immunocompetent hosts, cover a wide range of tumor types and are cost-effective (13). The main disadvantages of these models are that the tumour cells have to be implanted. Thus tumor growth may progress differently. Here, certain genetically engineered models have their advantages. In these models, the murine genome has been modified to change the function of genes which are involved in tumor development. Therefore the animals develop tumors spontaneously. The models are convenient if tumor development is to be followed from early time points on (14). Breeding and maintaining a colony large enough to generate sufficient numbers of mice of the same age and gender can be very difficult and costly (13).

The development of human tumor xenograft models also generated powerful tools for oncological research (15). In these models, human tumor cells are transplanted into immunodeficient animals. Historically, Rygaard and Povlsen realized the first successful transplantation of a human tumor in mice in 1969 (16). Since then, the model has been improved significantly. One main concern regarding both syngenic and xenograft models, is the difficulty of visualizing and quantifying the molecular events involved in tumor progression and dissemination. Labelling of tumor cells with fluorescent proteins has made a great contribution to overcome this problem.

Conventional Tumor Cell Quantification

Sensitive quantification of the tumor load in different animal organs is essential in order to monitor the development of tumor metastasis and to identify the treatment effect of different antitumoral drugs (17). However there are currently only few animal models that allow quantification of tumor load in a whole organ. These methods are based mostly on the staining of tumor in histological sections or fluorescence activated cell sorting (FACS)-analysis of live cell suspensions after tissue dissociation. These are often performed in only few sections of the relevant organ, which may be misleading, since an equal distribution of tumor cells within an organ is unlikely (18). Alternatively, preparation of cell suspensions for FACS-analysis may be performed, which involves many destructive steps, such as enzymatic tissue digestion by perfusion, organ mincing and filtering of the suspension through gauzes, which may lead both to the loss of tumor and healthy cells.

Accurate tumor cell quantification is particularly important in early tumor development since the size of micrometastases and the number of tumor cells arrested in the target organs can be very small. They can therefore evade conventional staining methods. Quantitative estimation of metastasis was typically based on the formation of macroscopic metastatic nodules. However, there are also tumor models in which organs are also diffusely infiltrated by scattered metastatic cells (18). To estimate the tumor load at early tumor stages in the case of diffuse metastasis, molecular techniques have been widely used for the detection of tumor cells. Polymerase chain reaction (PCR) was shown to be superior to conventional techniques in detecting occult tumor cells, allowing the identification of one malignant cell mixed with up to 10 million normal cells (19). A major strategy for the detection of occult tumor cells in the clinical context is PCR amplification of tumor-specific abnormalities present in the DNA or mRNA of these cells, such as tumor antigens. Recently, quantification of colorectal cancer metastasis in lymph nodes has been reported based on detection of tumor markers such as the carcinoembryonic antigen (CEA) by RT-PCR (20). The transfection of tumor cells with fluorescent proteins such as green fluorescent protein (GFP) allows for easy tumor quantification since the amount of GFP-marker protein mRNA will always correlate with the tumor load within the studied organ. Furthermore, it allows for easy visualization of the tumor.

GFP and its Variants

The cloning and heterologous gene transfer of wild-type GFP from the jellyfish *Aequorea victoria* brought about a revolution in cell biology. *GFP* cDNA encodes a 238 amino acid polypeptide that requires no other co-factors or substrates to fluoresce (21). As a fully genetically encoded label that can be linked with almost any protein, GFP has become a unique tool that enables direct visualization of cells and subcellular structures. Nowadays, advances in multiphoton fluorescent microscopy and the engineering of GFP into mutants with improved properties and altered colors have provided the basic tools that allow not only the direct visualization of cellular components, but also the quantification of signaling molecules and events with high spatial and temporal resolution in individual cells, both *in vitro* and *in vivo* (22). Especially in the Anthozoans (*e.g.* sea anemones), new fluorescent proteins have been exploited and modified through random site-directed mutagenesis. Recently the two-photon absorption spectra of over 48 fluorescent proteins, from enhanced BFP- (blue) and CFP- (cyan) series, the 'fruit' fluorescent proteins (*e.g.* mBanana, mOrange, tdTomato) to far-red variants, such as mRaspberry, mKate and Katushka2, have been characterized (23). Further modifications of these will lead to brighter mutants with improved properties for multiphoton applications. However, besides overall brightness, there are other factors of concern

such as folding dynamics, monomerization, and greater photostability. Due to their long-wavelength emission, the next-generation sensors with emission peaks in the far red spectrum are of special interest for *in vivo* imaging.

The Use of GFP in Tumor Models

GFP was the first fluorescent protein to be used for visualization of Chinese hamster ovary cells that were implanted orthotopically in nude mice (24). Chishima *et al*. stably transfected cancer cells with GFP and transplanted them into several mouse models. As a result, visualization of single metastatic cells in the tissues was possible for the first time without involvement of any post mortem histological technique (Figure 1). The recent explosion in the diversity of fluorescent proteins and a better understanding of their functionality under physiological conditions, allowed development of a variety of *in vivo* application modalities. Nowadays, fluorescent proteins can be used to visualize any type of cancer process, including primary tumor growth, tumor cell motility and invasion, metastatic seeding and colonization, angiogenesis, and the interaction between the tumor and its microenvironment (25). Transfected cell lines have been used to study tumor–host interaction, tumor immunology and tumor angiogenesis. Transfection of tumor cells with GFP allows *in vivo* observation of their fate in living organisms by video microscopy (17, 26). Here, mouse models with syngenic EGFP-transfected colon cancer cells, imitated the portal metastatic route and allowed intravital observation by intravital microscopy. Circulating tumor cells were easily monitored. Thus it was possible to monitor the tumor cell arrest within the liver vasculature which preceeded the tumor cell invasion (17, 27). These models permit real time, as well as post mortem observation of the pathophysiological processes involved in metastatic cancer growth and serve as a tool for monitoring the specific key steps of the metastatic cascade at the single-cell level. Therefore, these models can be used to clarify cell biological interactions and signalling cascades which are involved in the multistep process of tumor dissemination (17, 28). Importantly, not only the fluorescent attributes but also the number of DNA copies can be used as a marker to determine the effectiveness of novel therapeutic approaches (29, 30).

GFP-based Biological Sensors

Beside 'passive' fluorescent reporters for the measurement of protein expression, localization, and tracking within live cells, recent advances in the development of 'active' markers allow the monitoring of more complex cellular processes such as second messenger dynamics (*e.g.* Ca^{2+}, cAMP), receptor or enzyme activation and protein-protein interaction. For example all known second messengers are small molecules without complex structural features. They mediate a wide spectrum of cellular responses such as the regulation of proliferation, metabolism, cell migration, and/or cell death. Notably, impaired calcium signaling has recently been implicated in tumor cell migration and development of a metastatic cell phenotype (31). However, different signals might arise within one cell at the same time, rendering it necessary for the cell to achieve signal specificity. Clearly, as in the case of intracellular calcium, this specificity can be attributed to amplitude, pattern (*e.g.* oscillations), and subcellular compartmentalization of signals. Due to the de-differentiation of cells under two-dimensional culture conditions, the latter can only be imperfectly reconstituted *in vitro* in a reliable manner, making it necessary to study such processes in the context of an intact organism. The use of fluorescent protein-based sensors can now deliver such insights into many second messenger-dependent processes *in vitro* and *in vivo* (21, 32, 33). Most probes for the measurement of such dynamics show an environment-dependent change in their spectral characteristics. The most commonly used approach to monitor *e.g.* calcium, cAMP signaling and protein-protein interactions exploit Förster resonance energy transfer (FRET), usually between cyan and yellow fluorescent proteins, to transform conformational changes in the sensor molecule into measurable changes in their fluorescence spectra (*e.g.* Cameleon-based calcium sensors, RIα-EPAC-based sensors for cAMP). These sensors can be targeted to subcellular compartments and their ratiometric nature ensures that changes in probe quantity and movement artifacts are inherently corrected. Different types of FRET imaging can be applied, but not all of them can be easily used for quantitative measurements. As such, FRET-fluorescent lifetime imaging microscopy (FLIM) might be the most quantitative, but it is still fairly slow and, at least to our knowledge, has not yet been described in living organisms. Although it is not as quantitative as FLIM, we used dynamic ratiometric FRET-FLIM imaging, which relies on increased FRET acceptor (YFP) emission at the expense of donor (CFP) emission upon donor excitation, when FRET efficiency is rising. A good example are sensors based on EGFP and tHcred1 which we have recently developed for a functional imaging of caspase-3 activity. These sensors allowed monitoring of caspase-3 activation in cells by FRET-FLIM imaging microscopy or fluorescence correlation spectroscopy (34). The construct is based on EGFP and tHcred1 and a 14-amino acid linker containing the caspase-3 cleavage site for readout of apoptotic activity in cancer cells by FRET-FLIM (Figure 2). FRET between EGFP and tHcred1 in intact sensor, results in reduction of fluorescence lifetime of the donor–EGFP. This reduction can be correctly and reproducibly detected by FLIM microscopy. Activation of caspase-3 in the process of apoptosis disrupts the covalent linkage between EGFP and tHcred1 and effectively

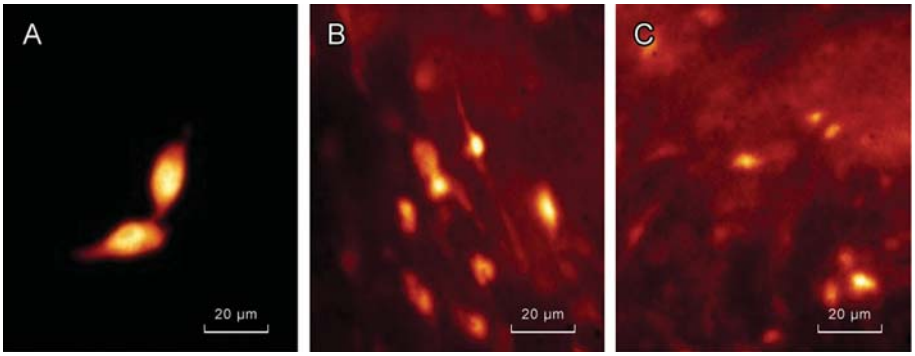

Figure 1. *EGFP-transfected tumor cells in cell culture (A) and in a mouse model of peritoneal (B) and hepatic metastases (C). Peritoneal metastases were generated by injecting EGFP-transfected C26 murine colon carcinoma cells (1×10^6 cells in 0,5 ml PBS) into the peritoneal cavity. To produce liver metastases the same number of cells were injected into the portal vein in 100 µl PBS. Mice were anesthetized by i.p. injection of 16 mg/kg Rompun® and 120 mg/kg Hostaket® (ketamine) and a midline laparotomy was performed after sterilization with iodine and alcohol swabs. The portal vein was exposed by retracting the intestines laterally and the cell suspension was slowly and carefully injected into the portal vein. Cells were easily detected by their fluorescence via intravital microscopy.*

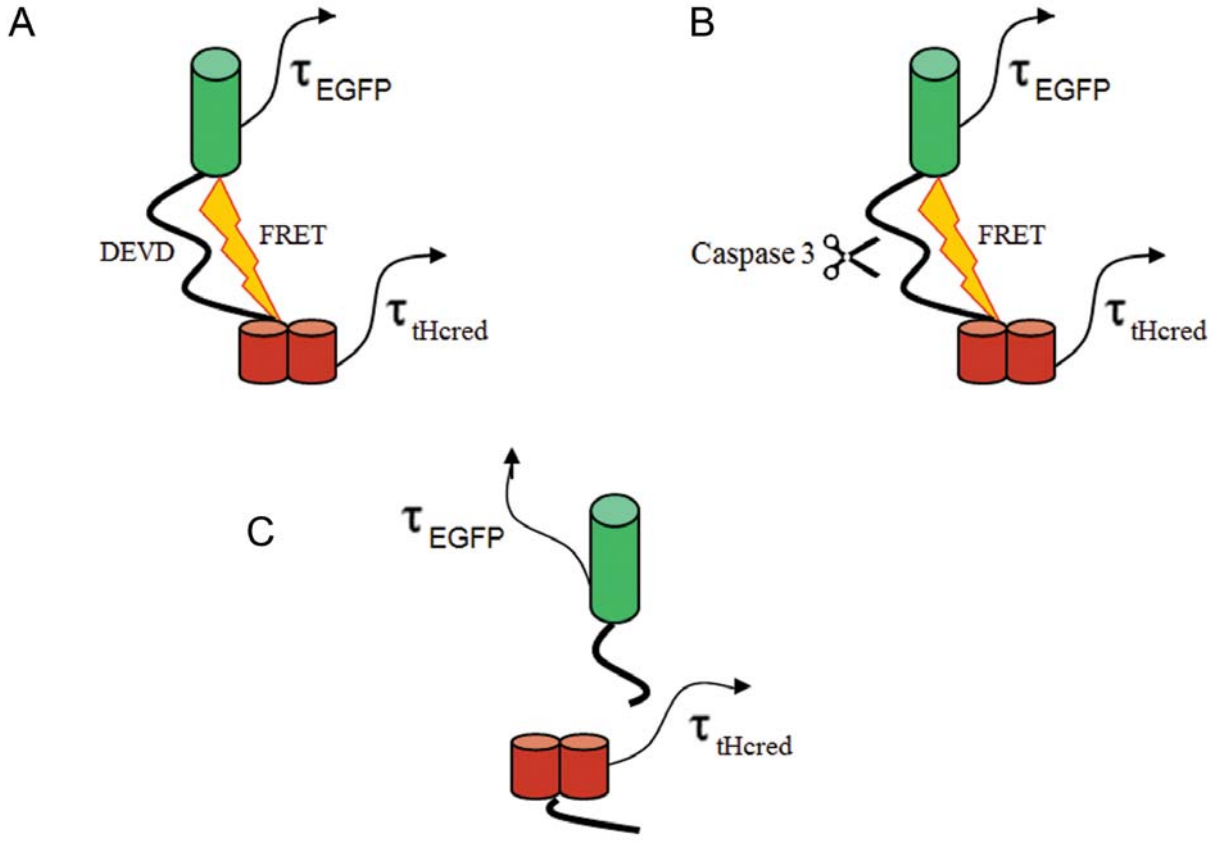

Figure 2. *Scheme of the (tHcred1-DEVD-EGFP) construct. A: The construct is in an intact state; FRET occurs between EGFP and tHcred1, reducing the EGFP fluorescence intensity and fluorescence lifetime. B: Apoptosis induction leads to caspase-3 activation in the cell. C: The sensor is cleft, leading to no FRET between the two chromophores; consequently the EGFP florescence intensity and fluorescence lifetime will be increased compared to that of intact construct.*

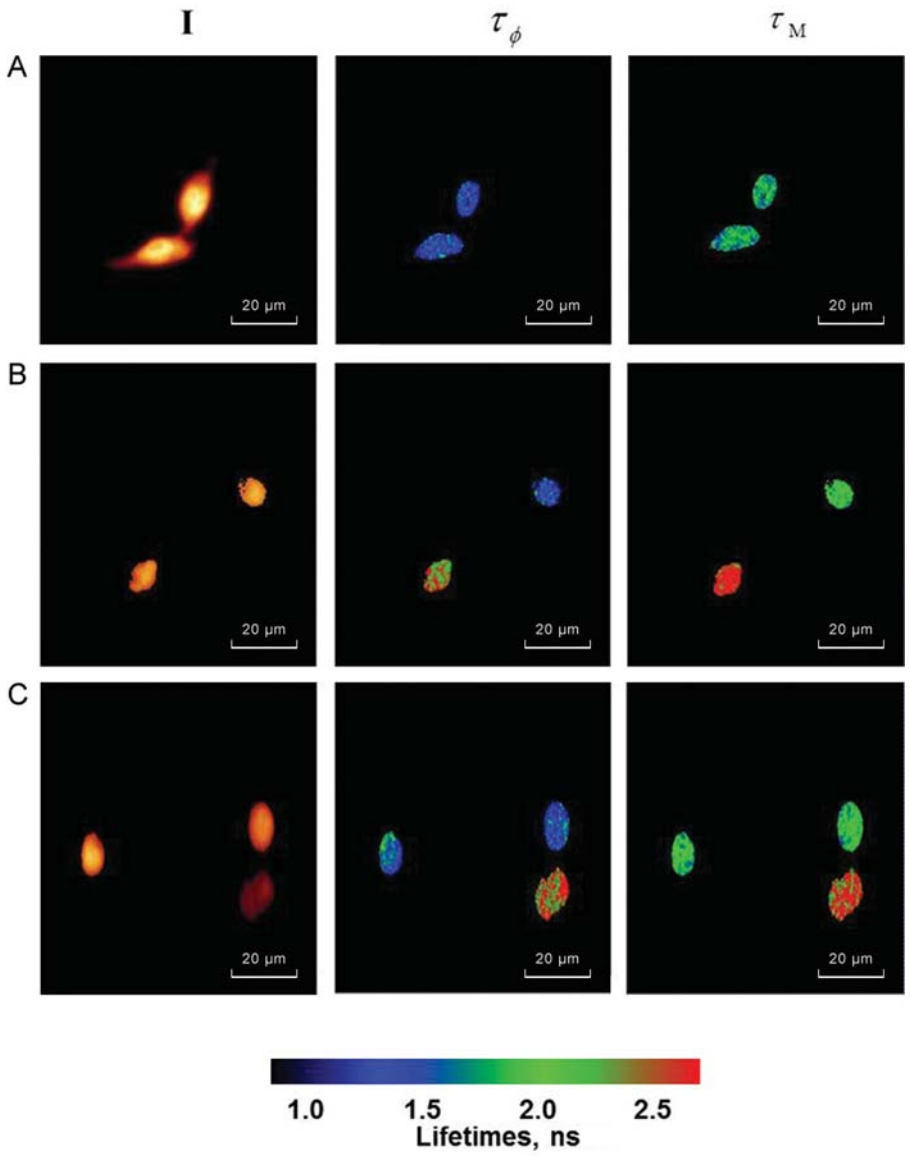

Figure 3. *Representative FRET-FLIM images from different treatment groups. Fluorescence intensity (I), phase lifetime (τ phase) and modulation lifetime (τ mod) images are shown. The calibration bar below the figure shows values for EGFP fluorescence lifetimes. A: Untreated C26 cells (τ phase 1.74 ns and 1.76 ns; τ mod 1.94 ns and 1.93 ns respectively). B: Cells treated with 5FU for 24 h (τ phase 1.82 ns and 2.33 ns; τ mod 2.1 ns and 2.46 ns respectively). C: Cells treated by 5FU for 48 h (τ phase 1.82 ns, 1.8 ns and 2.4 ns; τ mod 2.08 ns, 2.11 ns and 2.52 ns respectively).*

eliminates FRET, thus conveying that a cell is apoptotic. EGFP phase lifetimes of 1,6-2.0 ns means cells are considered as being healthy, and longer than 2.0 ns as being apoptotic (Figure 3). Sensor (tHcred1-DEVD-EGFP)-transfected colorectal tumor cells such as SW-480 cells, can be used for reproducible single-cell-based apoptosis detection and quantification (34).

Using this biosensor for caspase-3 activity and apoptosis, we transferred this approach to a mouse model of peritoneal and liver metastasis (35). For this, the tHcred1-DEVD-EGFP construct was stably transfected into C26 murine colon-carcinoma cells. These cells were then implanted by intra-portal and intraperitoneal injection into syngenic Balb/c mice to generate models for liver and peritoneal metastasis.

Capase-3 sensor also allowed quantification of the apoptosis rate in fresh tumor tissue samples derived from peritoneal and liver metastases. Besides these *in vivo* measurements, apoptosis can also be measured in an *ex vivo* setting (Figure 4). For this purpose, sensor-transfected C26 cells were isolated from omental tissue of the tumor-bearing

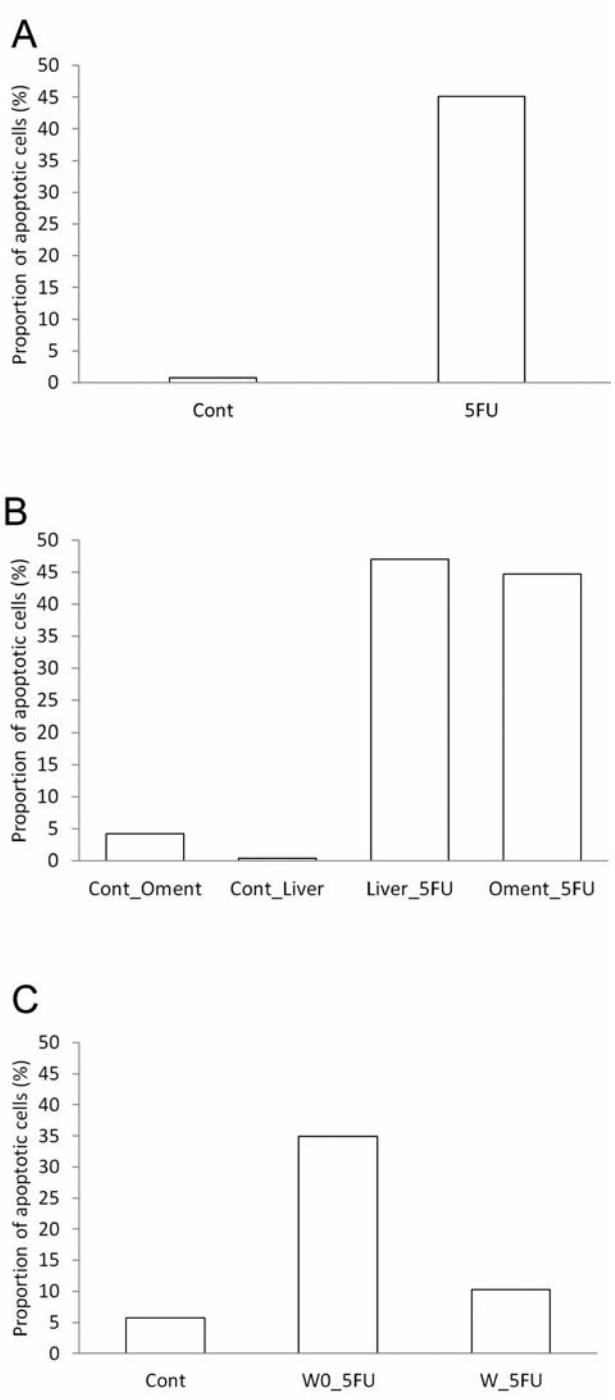

Figure 4. *Apoptosis rate was determined in (tHcred1-DEVD-EGFP)-transfected C26 cells by (FLIM) (n=120) under in vitro (A), in vivo (B) and ex vivo conditions (C). In vitro: cells were treated with 25 μM 5FU. In vivo: Oment_5FU and Liver_5FU are the apoptosis rate in the fresh tissue samples from mouse models of omental and livermetastasis. These animals were not treated by 5FU, therefore the cells remained responsive to 5FU. Ex vivo: WO_5FU is the apoptosis rate after exposure to 5FU treatment in cells which were extracted from omental tissue of non 5FU-treated animals; W_5FU shows further 5FU treatment of cells from omental tissue of mice initially treated with 5FU.*

mice and were studied further under cell culture conditions. The cells were isolated both from 5FU-treated and non-treated mice. Further 5FU treatment of the cells derived from 5FU-treated mice have caused significantly less apoptosis, than treating intact sensor containing cells and cells isolated from non-treated mice. We have explained this phenomenon with increasing resistance of the cells towards longer treatment with 5FU in mice. Since tHcred1-DEVD-EGFP transfection of C26 cells allowed an accurate quantification of the apoptosis rate in response to chemotherapy, the model provided a platform for chemoresistance studies. Furthermore, it was possible to measure the tumor load in the whole organ through real-time PCR quantification of EGFP DNA copies. Directly after removing organs, DNA was extracted from the omentum and the liver using a modified DNA purification protocol. Tumor load was determined by real-time PCR for EGFP with the genomic DNA (Figure 5).

Tumor load determination in the liver and omental tissues demonstrated the effect of chemotherapy. Under ongoing 5FU treatment, the tumor load in omentum decreased at 72 h compared to the control and the previous treatment time point. Interestingly, after 240 h of treatment, the tumor load again significantly increased. This is likely due to increasing chemoresistance to 5FU, which correlated with the FLIM data.

In summary, the novel fluorescent protein sensor allowed quantification of apoptosis and of the tumor load in omental and liver metastases of colorectal cancer in the mouse. Using this model, we are currently investigating different therapeutic approaches to overcome resistance development and to study the ways of overcoming the resistance.

Future Perspectives

Advances in microscopy and optical imaging and the generation of new fluorescent biosensors have revolutionized optical imaging. Live cell imaging has been used to study a variety of cells in different organisms. Optical imaging of specific molecular targets and pathways in living cells has recently become possible through continued developments in microscopic imaging technology, and more importantly, due to the availability of genetically encoded fluorescent biosensors (36-38). Rational genetic engineering of GFP molecules will in future lead to further evolution in terms of brightness and biocompatibility (39). These fluorescent reporters have already further promoted live-cell imaging of biochemical processes in a variety of cells from different organisms (37, 40). Interactions between two or more proteins are presently used to study protein reactions in living cells by FRET (41, 42) within living cells. The development of new and brighter mutants in the blue (43) and in the red region of the light spectrum (44) will enable the development of new biosensors with a significantly enhanced FRET efficiency. Quantitative co-expression of two or more proteins has

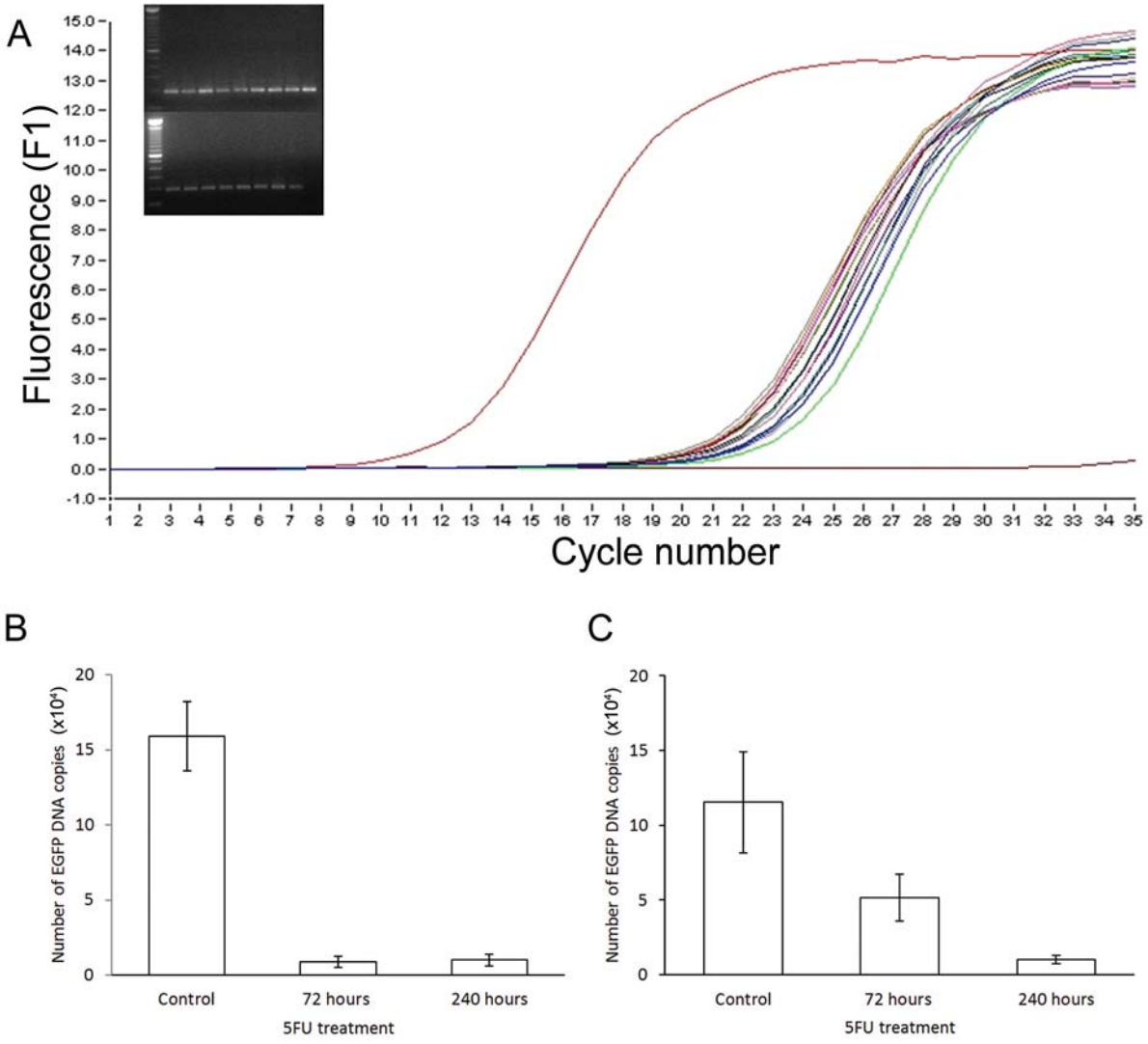

Figure 5. *Tumor load quantification in liver and omental tissue. A: EGFP melting curve. B: Tumor load in omental tissue after treatment of mice with 30 mg/kg (5FU). C: Tumor load in liver tissue after treatment of mice with 30 mg/kg 5FU. Tumor load determination in liver metastases also demonstrated the treatment effect of 5FU at 72 and 240 h. At these time points, the tumor loads had decreased significantly compared to the control. To quantify EGFP-DNA copies in samples of the above-mentioned preparations, LightCycler quantification was applied. To purify genomic DNA from tissue samples, we developed a protocol on the basis of the QIAamp DNA Mini tissue protocol. We first measured the weight of the whole organ sample and then added 80 μl of PBS for each 25 mg of tissue. Tissues were homogenized mechanically. After homogenization we took 100 μl of homogenate and added 100 μl of lysis (ATL) buffer and the standard QIAamp DNA Mini tissue purification protocol was carried out. Real time (PCRs) were carried out using LightCycler FastStart DNA Master SYBR Green I. The reaction mixture consisted of 2 μl of LightCycler FastStart DNA Master SYBR Green I (FastStart Taq DNA polymerase, reaction buffer, dNTP mixture (with dUTP instead of dTTP), SYBR Green I dye and 10 mM MgCl2), 2.4 μl of 25 mM $MgCl_2$, 0.5 mM of EGFP-specific primers, (5'-TAC GGC AAG CTG ACC CTG AAG TTC-3' (sense) and 5'-CGT CCT TGA AGA AGA TGG TGC-3' (antisense)) and 2 μl of DNA derived from different preparations. The cycling program consisted of 600 s initial denaturation at 95˚C, 7 s 95˚C denaturation, 64˚C annealing for 5 s, and 72˚C extension for 10 s with a transition rate of 20˚C/s between temperature plateaus for a total of 35 cycles. Quantification data was analyzed using LightCycler analysis software version 3.5. As standard, the plasmid tHcred1-DEVD-EGFP cDNA was used. The second derivative maximum method analysis algorithm was chosen for generating the standard curve. The error point was <0.1, the slope <3.3 Cp and the regression coefficient was r=1.00. PCR products were analyzed on a 1% agarose gel to ensure specifity.*

recently been achieved with little cell-to-cell variability. This finding enables reliable co-expression of donor and acceptor-tagged proteins for FRET studies, which is of particular importance for the development of novel biomolecular sensors that can be expressed from a single plasmid (43). Advances in microscopy such as *in vivo* two- photon FLIM microscopy will permit monitoring of the parallel function of two or more biosensors within a living tumor animal model.

References

1 Stock CC, Reilly HC, Buckley SM, Clarke DA and Rhoads CP: Azaserine, a new tumour-inhibitory substance; studies with Crocker mouse sarcoma 180. Nature *173*: 71-72, 1954.

2 Maltman DJ and Przyborski SA: Developments in three-dimensional cell culture technology aimed at improving the accuracy of *in vitro* analyses. Biochem Soc Trans *38*: 1072-1075, 2010.

3 Brown JM and Giaccia AJ: The unique physiology of solid tumors: opportunities (and problems) for cancer therapy. Cancer Res *58*: 1408-1416, 1998.

4 Burchill SA: What do, can and should we learn from models to evaluate potential anticancer agents? Future Oncol *2*: 201-211, 2006.

5 Yamada KM and Cukierman E: Modeling tissue morphogenesis and cancer in 3D. Cell *130*: 601-610, 2007.

6 Staton CA, Stribbling SM, Tazzyman S, Hughes R, Brown NJ and Lewis CE: Current methods for assaying angiogenesis *in vitro* and *in vivo*. Int J Exp Pathol *85*: 233-248, 2004.

7 Vailhe B, Vittet D and Feige JJ: *In vitro* models of vasculogenesis and angiogenesis. Lab Invest *81*: 439-452, 2001.

8 Nguyen M, Shing Y and Folkman J: Quantitation of angiogenesis and antiangiogenesis in the chick embryo chorioallantoic membrane. Microvasc Res *47*: 31-40, 1994.

9 Ausprunk DH, Knighton DR and Folkman J: Vascularization of normal and neoplastic tissues grafted to the chick chorioallantois. Role of host and preexisting graft blood vessels. Am J Pathol *79*: 597-618, 1975.

10 Griswold DP Jr. and Harrison SD Jr.: Tumor models in drug development. Cancer Metastasis Rev *10*: 255-261, 1991.

11 Sporn MB and Liby KT: Cancer chemoprevention: scientific promise, clinical uncertainty. Nat Clin Pract Oncol *2*: 518-525, 2005.

12 Darro F, Decaestecker C, Gaussin JF, Mortier S, Van Ginckel R and Kiss R: Are syngeneic mouse tumor models still valuable experimental models in the field of anti-cancer drug discovery? Int J Oncol *27*: 607-616, 2005.

13 Teicher BA: Tumor models for efficacy determination. Mol Cancer Ther *5*: 2435-2443, 2006.

14 Hanahan D: Heritable formation of pancreatic beta-cell tumours in transgenic mice expressing recombinant insulin/simian virus 40 oncogenes. Nature *315*: 115-122, 1985.

15 Peterson JK and Houghton PJ: Integrating pharmacology and *in vivo* cancer models in preclinical and clinical drug development. Eur J Cancer *40*: 837-844, 2004.

16 Rygaard J and Povlsen CO: Heterotransplantation of a human malignant tumour to "Nude" mice. Acta Pathol Microbiol Scand *77*: 758-760, 1969.

17 Sturm JW, Keese MA, Petruch B, Bonninghoff RG, Zhang H, Gretz N, Hafner M, Post S and McCuskey RS: Enhanced green fluorescent protein-transfection of murine colon carcinoma cells: key for early tumor detection and quantification. Clin Exp Metastasis *20*: 395-405, 2003.

18 Kruger A, Umansky V, Rocha M, Hacker HJ, Schirrmacher V and von Hoegen P: Pattern and load of spontaneous liver metastasis dependent on host immune status studied with a lacZ transduced lymphoma. Blood *84*: 3166-3174, 1994.

19 Ghossein RA, Bhattacharya S and Rosai J: Molecular detection of micrometastases and circulating tumor cells in solid tumors. Clin Cancer Res *5*: 1950-1960, 1999.

20 Ho SB, Hyslop A, Albrecht R, Jacobson A, Spencer M, Rothenberger DA, Niehans GA, D'Cunha J and Kratzke RA: Quantification of colorectal cancer micrometastases in lymph nodes by nested and real-time reverse transcriptase-PCR analysis for carcinoembryonic antigen. Clinical cancer research: an official journal of the American Association for Cancer Research *10*: 5777-5784, 2004.

21 Chudakov DM, Matz MV, Lukyanov S and Lukyanov KA: Fluorescent proteins and their applications in imaging living cells and tissues. Physiol Rev *90*: 1103-1163, 2010.

22 Zhang J, Campbell RE, Ting AY and Tsien RY: Creating new fluorescent probes for cell biology. Nat Rev Mol Cell Biol *3*: 906-918, 2002.

23 Drobizhev M, Makarov NS, Tillo SE, Hughes TE and Rebane A: Two-photon absorption properties of fluorescent proteins. Nature methods *8*: 393-399, 2011.

24 Chishima T, Miyagi Y, Wang X, Yamaoka H, Shimada H, Moossa AR and Hoffman RM: Cancer invasion and micrometastasis visualized in live tissue by green fluorescent protein expression. Cancer Res *57*: 2042-2047, 1997.

25 Hoffman RM: The multiple uses of fluorescent proteins to visualize cancer *in vivo*. Nat Rev Cancer *5*: 796-806, 2005.

26 Al-Mehdi AB, Tozawa K, Fisher AB, Shientag L, Lee A and Muschel RJ: Intravascular origin of metastasis from the proliferation of endothelium-attached tumor cells: a new model for metastasis. Nat Med *6*: 100-102, 2000.

27 Hayashi K, Kimura H, Yamauchi K, Yamamoto N, Tsuchiya H, Tomita K, Kishimoto H, Hasegawa A, Bouvet M and Hoffman RM: Comparison of cancer-cell seeding, viability and deformation in the lung, muscle and liver, visualized by subcellular real-time imaging in the live mouse. Anticancer Res *31*: 3665-3672, 2011.

28 Suetsugu A, Katz M, Fleming J, Truty M, Thomas R, Saji S, Moriwaki H, Bouvet M and Hoffman RM: Imageable Fluorescent Metastasis Resulting in Transgenic GFP Mice Orthotopically Implanted with Human-patient Primary Pancreatic Cancer Specimens. Anticancer Res *32*: 1175-1180, 2012.

29 Zhou W, Zhu H, Chen W, Hu X, Pang X, Zhang J, Huang X, Fang B and He C: Treatment of patient tumor-derived colon cancer xenografts by a TRAIL gene-armed oncolytic adenovirus. Cancer Gene Ther *18*: 336-345, 2011.

30 Keese M, Gasimova L, Schwenke K, Yagublu V, Shang E, Faissner R, Lewis A, Samel S and Lohr M: Doxorubicin and mitoxantrone drug eluting beads for the treatment of experimental peritoneal carcinomatosis in colorectal cancer. International journal of cancer. Journal international du cancer *124*: 2701-2708, 2009.

31 Prevarskaya N, Skryma R and Shuba Y: Calcium in tumour metastasis: new roles for known actors. Nat Rev Cancer *11*: 609-618, 2011.

32 Choi KR, Berrera M, Reischl M, Strack S, Albrizio M, Roder IV, Wagner A, Petersen Y, Hafner M, Zaccolo M and Rudolf R: Rapsyn mediates subsynaptic anchoring of PKA type I and stabilisation of acetylcholine receptor *in vivo*. J Cell Science *125*: 714-723, 2012.

33 Rudolf R, Hafner M and Mongillo M: Investigating second messenger signaling *in vivo*. Methods in enzymology *505*: 363-382, 2012.

34 Keese M, Offterdinger M, Tischer C, Girod A, Lommerse PH, Yagublu V, Magdeburg R and Bastiaens PI: Quantitative imaging of apoptosis commitment in colorectal tumor cells. Differentiation 75: 809-818, 2007.
35 Keese M, Yagublu V, Schwenke K, Post S and Bastiaens P: Fluorescence lifetime imaging microscopy of chemotherapy-induced apoptosis resistance in a syngenic mouse tumor model. International journal of cancer. J International du Cancer *126*: 104-113, 2010.
36 Heim R and Tsien RY: Engineering green fluorescent protein for improved brightness, longer wavelengths and fluorescence resonance energy transfer. Curr Biol *6*: 178-182, 1996.
37 Welsh DK and Kay SA: Bioluminescence imaging in living organisms. Curr Opin Biotechnol *16*: 73-78, 2005.
38 Funovics M, Weissleder R and Tung CH: Protease sensors for bioimaging. Anal Bioanal Chem *377*: 956-963, 2003.
39 Goedhart J, von Stetten D, Noirclerc-Savoye M, Lelimousin M, Joosen L, Hink MA, van Weeren L, Gadella TW Jr. and Royant A: Structure-guided evolution of cyan fluorescent proteins towards a quantum yield of 93%. Nat Commun *3*: 751, 2012.
40 Rhee JM, Pirity MK, Lackan CS, Long JZ, Kondoh G, Takeda J and Hadjantonakis AK: *In vivo* imaging and differential localization of lipid-modified GFP-variant fusions in embryonic stem cells and mice. Genesis *44*: 202-218, 2006.
41 Chen Y, Mills JD and Periasamy A: Protein localization in living cells and tissues using FRET and FLIM. Differentiation *71*: 528-541, 2003.
42 Bastiaens PI and Squire A: Fluorescence lifetime imaging microscopy: spatial resolution of biochemical processes in the cell. Trends Cell Biol *9*: 48-52, 1999.
43 Goedhart J, van Weeren L, Hink MA, Vischer NO, Jalink K and Gadella TW Jr.: Bright cyan fluorescent protein variants identified by fluorescence lifetime screening. Nat Methods *7*: 137-139, 2010.
44 Muller-Taubenberger A and Anderson KI: Recent advances using green and red fluorescent protein variants. Appl Microbiol Biotechnol *77*: 1-12, 2007.

Received May 16, 2012
Revised June 3, 2012
Accepted June 5, 2012